Study on the Crevice Corrosion Behavior of 316L Stainless Steel used on Marine Gas Turbine Inlet Filters by Stochastic Methods

Zhongyi Wang[1], Yuan Cong[2], Tao Zhang[2,3,*], Yawei Shao[2,3], Guozhe Meng[2,3]

[1] College of Power and Energy Engineering, Harbin Engineering University, Nantong ST 145, Harbin, 150001, China
[2] Corrosion and protection Laboratory, Key Laboratory of Superlight Materials and Surface Technology (Harbin Engineering University), Ministry of Education, Nantong ST 145, Harbin, 150001, China
[3] State Key Laboratory for Corrosion and Protection, Institute of Metal Research, Chinese Academy of Sciences, Wencui RD 62, Shenyang, 110016, China)
[*]E-mail: zhangtao@hrbeu.edu.cn

The crevice corrosion behavior of 316L stainless steel (316L SS) which used on marine gas turbine inlet filters was investigated in 3.5% NaCl solution by means of potentiodynamic polarization and potentiostatic technology, and the experimental data were analyzed on the basis of stochastic theory. The presence of crevice deteriorated the corrosion resistance of 316L SS, distinguished by the decrease of breakdown potential. The results also demonstrated that crevice had three effects on the corrosion behavior of 316L SS: (1) crevice hindered the passive film formation rate; (2) crevice had great influence on the metastable corrosion initiation process; (3) the presence of crevice increased the stable corrosion growth probability, the stable corrosion was easy to grow up with a higher growth rate, and finally spread over the covered surface.

1. INTRODUCTION

Recently, stochastic and statistic approach has been applied on the study of localized corrosion (pitting corrosion, crevice corrosion). Localized corrosion comprises two main processes: corrosion initiation and corrosion growth.

As in the case of corrosion initiation, the exponential distribution has been confirmed for the distribution of initiation time [1, 2]. Based on these results, stochastic pit generation models have been

proposed in literature based on the homogeneous Poisson process [1]. Shibata et al. [3] has made clear that lifetime estimation of structures affected by localized corrosion is difficult unless the stochastic approach is introduced. A birth and death stochastic process model was developed to explain the statistical distribution of induction time for pit generation. Puyn and Kim [4-7] investigated the pitting corrosion of aluminum alloy using Weibull distribution function. Burstein et al. [8-10] studied the nucleation/ metastable pitting rate of stainless steel by statistic method.

As in the case of corrosion growth, Provan and Rodríguez [11] used a nonhomogeneous Markov process to model pitting depth growth for the first time. They compared the estimated results with the experimental data reported for aluminum by Aziz [12] and their own pitting corrosion experiences conducted on stainless steels. The combined effect of pit generation and growth was modeled by Hong as a combined stochastic process [13]. The use of the method was illustrated using the experimental data reported by Provan [11] and Aziz [12]. In recent years, important advances have been made in modeling the growth of localized corrosion through Markov chains [1, 14-16]. Bolzoni et al. [14] used a continuous-time, three-state Markov process to model the first stages of localized corrosion considering three possible states of the metal surface: passivity, metastability and localized corrosion. Valor et al. [1] proposed a new stochastic model in which pit initiation is modeled as a Weibull process, while pit growth is modeled using a non-homogenous, linear growth Markov process. Later, Zhang, Meng and Shao et al. used this stochastic model to investigate the corrosion susceptibility of Mg alloys [15], Nano-Al [16] and organic coating [17].

Crevice corrosion is still a very dangerous type of local corrosion and commonly occurs on passive materials. Inside small crevices, the electrolyte exchange is severely disabled and therefore the corrosion condition can be aggravating over time [18, 19]. In the last several decades, crevice corrosion was a hot topic for many scientists. As in the case of crevice corrosion can be subdivided into two major stages:[18, 19] (i) initial stage of corrosion, including oxygen depletion, acidification, nucleation or initiation of active sites on a passive metal and local breakdown of the passive oxide (ii) propagation or development of active sites. However, only a few studies have been reported on the stochastic process of crevice corrosion [20]. In order to introduce such a discussion on the crevice corrosion, the present work is aim to investigate the crevice corrosion behavior of 316L stainless steel (316L SS) based on stochastic and statistic methods.

2. EXPERIMENTAL

2.1. Materials

The material was 316L stainless steel (316L SS) whose main compositions were: 19.4% Cr, 11.8% Ni, 2.2% Mn, 2.4% Mo, 0.2% Si. The sample is the cylinder with the diameter of 10 mm. An artificial crevice was constructed according to ASTM standard G 48-97 [21], a plexiglas sheet of about 5mm thickness was attached to the electrode surface to form a crevice between plexiglas sheet and electrode surface (Fig.1). The ratio of crevice to bold surface area is about 1:5 and the crevice gap is about 20 μm..

All of the specimens were wet ground to a 2000-grit finish, degreased with acetone, rinsed with distilled water and dried in a compressed hot air flow. The test solution was 3.5% NaCl solution, which was prepared from analytical grade reagent and deionized water.
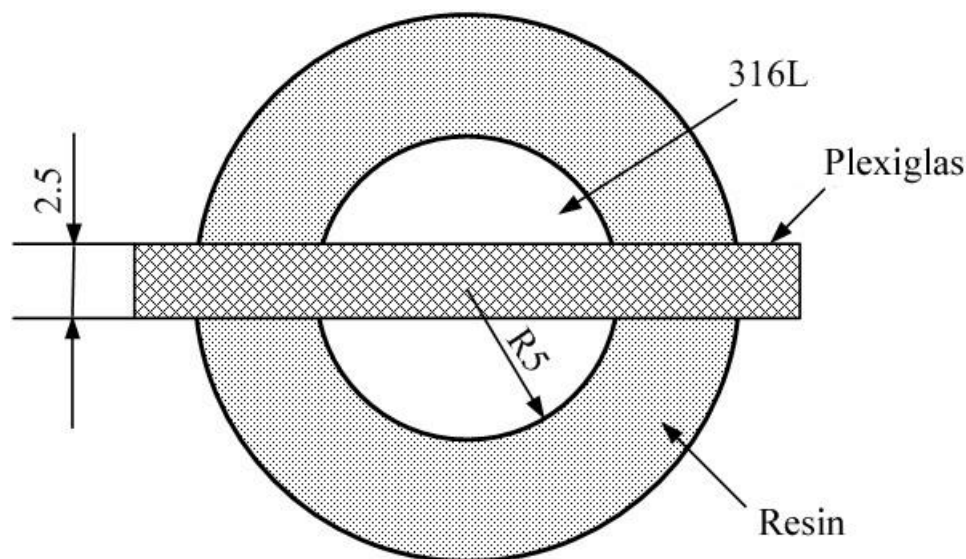

Figure 1. Schematic of the experimental setup for measuring crevice corrosion.

2.2. Electrochemical measurements

A three-electrode cell was used with a counter electrode of platinum (20mm×20mm) and an Ag/AgCl reference electrode.

For the polarization curve measurements, the specimens were studied at a scan rate of 0.333 mV/s. For the induction time measurements, the specimens were pretreated in NaCl solution at a constant potential, 90 $mV_{Ag/AgCl}$, for 1000s. After pretreatment, the specimens were immersed in the NaCl solution, and a potentiostatic technique (90 $mV_{Ag/AgCl}$) was used to measure the anodic current. The variation of anodic current as a function of the potentiostatic time was recorded with a data-sampling interval of 0.25 s. A sudden increase in the anodic current was observed. Such a current increase was the result of the onset of crevice corrosion, which was confirmed by morphological observation. The time interval for this sudden current increase is defined as the crevice corrosion induction time. The above experiments were carried out using a PAR273 Electrochemical Measurement System manufactured by EG&G.

2.3. Corrosion morphology observation

The corrosion morphology was observed after the removal of corrosion products. The corrosion products were removed using the chemical products-clean up method (idt ISO 8407:1991). Finally, the specimens were washed with deionized water, dried by hot air flow. The corrosion morphology of

316L SS in the presence and absence of crevice was observed by scanning electronic microscopy (CAMBRIDGE STEREOSCAN 240).

3. RESULTS AND DISCUSSION

3.1. Potentiodynamic polarization curves

The potentiodynamic polarization curves of 316L SS with and without crevice were illustrated in Fig.2. It was noted that the breakdown potential (E_b) of 316L SS without crevice was higher than that with crevice, which indicated that the corrosion resistance decreased in case of crevice.
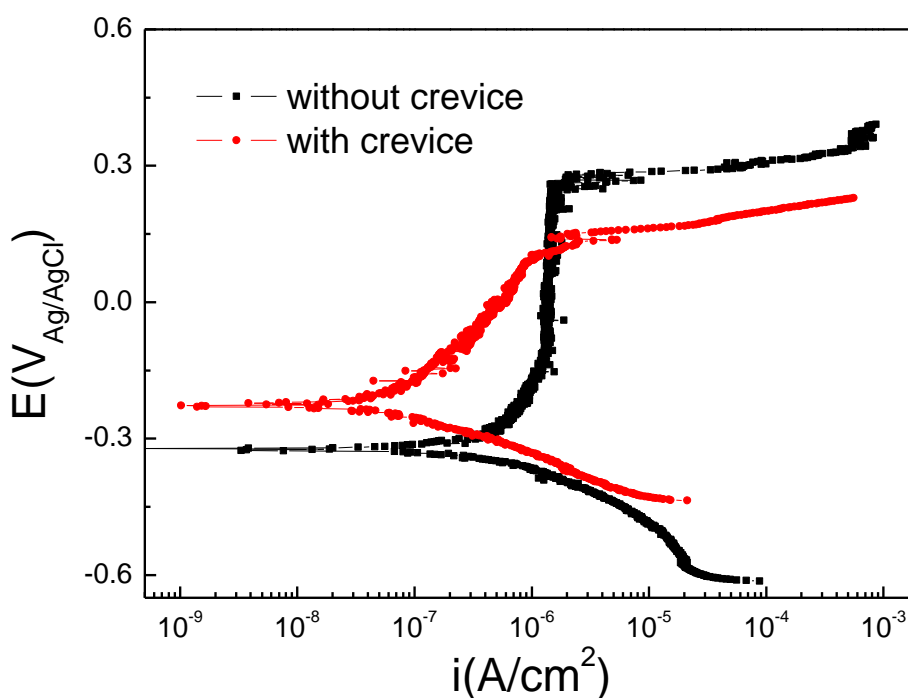

Figure 2. Potentiodynamic polarization curves of 316L SS with and without crevice.

3.2. Potentiostatic measurements

The current traces of 316L SS with and without crevice were given in Fig.3. It can be observed that there existed many spikes or fluctuations, which indicated the formation of passive film, generation, growth and repassivation of the matastable corrosion along the curves. All of the current traces could be distinguished three stages: passivation, metastable corrosion and stable corrosion

In order to obtain the detail information, the potentiostatic curves were re-plotted in Fig.4 by discounting the current trace of the stable corrosion stage. During the passivation stage, a current spike is observed, which consists of the charging of the electrochemical double layer and the nucleation process of passive film.

During the metastable corrosion stage, the current spikes included metastable corrosion generation and repassivation, which was random at a specific site distributed in a large number of possible active sites. Both current traces showed common features. First, they all showed electrochemical noise, irrespective of crevice. The current noise was existed only when the sample was in the anodic polarization and was a consequence of metastable corrosion. Second, both current traces shown displayed a decaying overall current, implying that the metal was passivating continuously, despite the periodic transient depassivation induced by metastable corrosion.
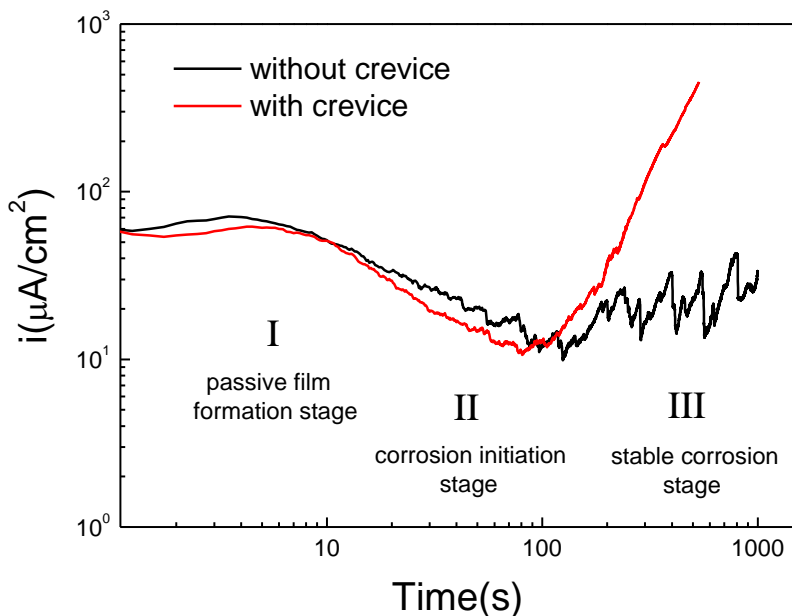

Figure 3. Potentiostatic current traces of 316L SS with and without crevice.
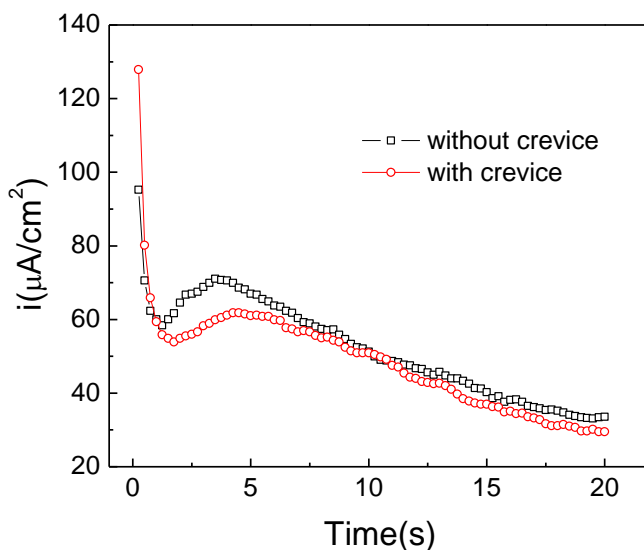

Figure 4. Re-plotted potentiostatic curves by discounting the current trace of the stable corrosion stage
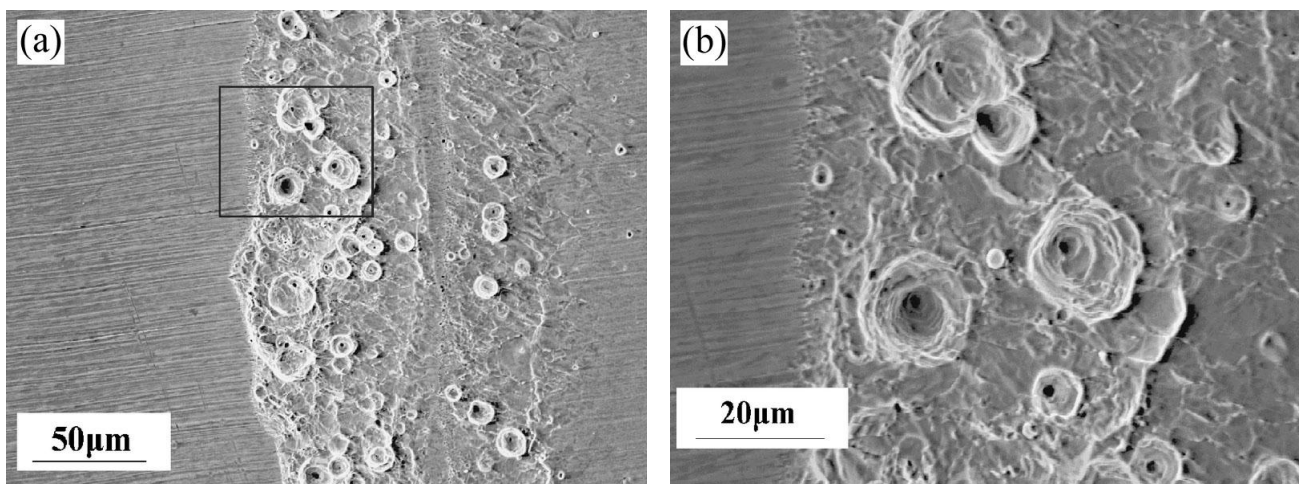
After induction time, the growth of metastable corrosion lead to marcro-corrosion, which was characterized by the current trace which did not return to the current baseline and had a gradual current increase (stable corrosion).

3.3. Crevice corrosion morphology

The macroscopic corrosion morphology of 316L SS with and without crevice after potentiostatic polarization were represented in Fig.5, where the sites coved by plexiglas sheet were corroded, while the other region of the specimens still remained their fresh surface.

Figure 5. The macroscopic corrosion morphology of 316L SS with and without crevice after potentiostatic polarization measurement.
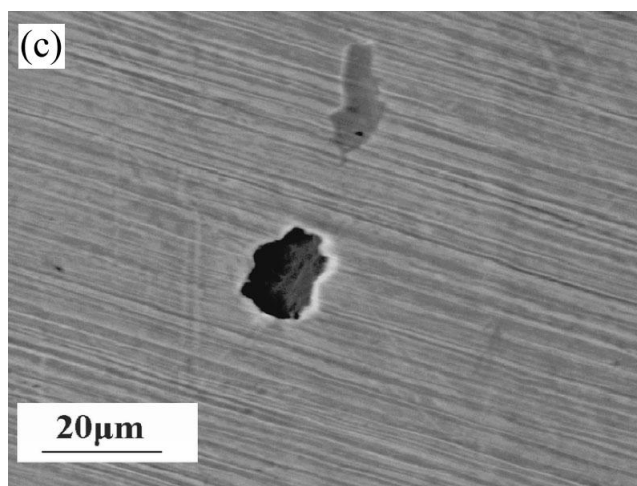
Figure 6. SEM images of corrosion morphology of 316L SS with **(a, b)**and without **(c)** crevice.

The specimens with and without crevice were examined in the SEM to obtain more detail information. Typical corrosion morphology was given in Fig.6. The corrosion morphology of 316L SS with crevice exhibited distinguishing feature with that without crevice.

4. DISCUSSION

4.1. Effect of crevice on the formation of passive film on 316L SS

From Fig.4, it can be seen that, each of the "current-time" curves consists of an initial spike (within the first 0.8 s) due to the charging of the electrochemical double layer [22, 23], a subsequently rising portion due to the nucleation process and a posterior decreasing portion due to the diffusion process. During this stage of the formation of the passive film, the nuclei develop diffusion zones around themselves and as these zones overlap the transient current decreases rapidly due to the poor electroconductance of the passive film and reach steady state current.

Considering the current transients observed in the course of the formation of passive films, a suitable model for the formation mechanism of passive film seems to be the overlapping of two growth steps. One step is instantaneous nucleation process, 2D growth, determined by the lattice incorporation onto the periphery of a growing nucleus and taking into account the overlap of nuclei [24]. The current-time transient for this instantaneous nucleation process had been shown [24, 25] as follows:

$$i_{2D} = \frac{2\pi n F M h N_0 k_g^2 t}{\rho} \exp[-\frac{\pi N_0 M^2 k_g^2 t^2}{\rho^2}] \qquad (1)$$

This equation predicts a maximum in the current-time curve with

$$t_m = (\frac{\rho^2}{2\pi N_0 M^2 k_g^2})^{1/2} \qquad (2)$$

and

$$i_m = nFhk_g(2\pi N_0)^{1/2}\exp(-\frac{1}{2}) \qquad (3)$$

The other step is progressive nucleation process, 3D growth, the nucleation of pyramids at a constant rate on the substrate which grow in three dimensions. The current–time transient for the case where the pyramids are of right circular cone type has been shown to be [26]:

$$i_{3D} = nFk_2[1-\exp(\frac{-\pi M^2 k_1^2 A t^3}{3\rho^2})]\exp(\frac{-\pi M^2 k_1^2 A t^3}{3\rho^2}) \qquad (4)$$

This predicts a maximum in the current–time curve with

$$t_m = (\frac{3\rho^2 \ln 2}{\pi M^2 k_1^2 A}))^{1/3} \qquad (5)$$

and

$$i_m = \frac{nFk_2}{4} \qquad (6)$$

In the above equations, N_0 is the number density of active sites, k_g is the lateral growth rate constant of nuclei, A is the nucleation rate constant, M is the molecular weight (160 g/mol), ρ is the density of the deposited material (Fe_2O_3 5.18 g/cm^3), h is the thickness of the deposited layer, k_1 and k_2 are the rate constants for parallel and perpendicular growth with respect to the electrode surface and nF refers to the molar charge transferred during the process.

In Fig.7, the non-dimensional i/i_m was plotted as a function of t/t_m, for the passive film formation of 316L SS with and without crevice. The experimental i/i_m–t/t_m curves seem to follow the theoretic progressive nucleation curve (3D) more closely whether with crevice or not, and which indicated progressive nucleation (3D) was more possible to proceed under that condition. In another word, crevice had no influence on the formation mechanism of passive film on 316L SS.

However, it was noticed that the t_m and i_m of 316L SS without crevice (4.25 s) was longer than that with crevice (3.5 s). The important kinetic parameters, AK_1^2 and K_2, represent the horizontal and vertical formation rate of passive film, were calculated according to progressive nucleation theoretical model (Eqn.5 and 6). [23]. In case of crevice, the value of AK_1^2 and K_2 decreased (table 1), which implied that the crevice hindered the formation rate of passive film.
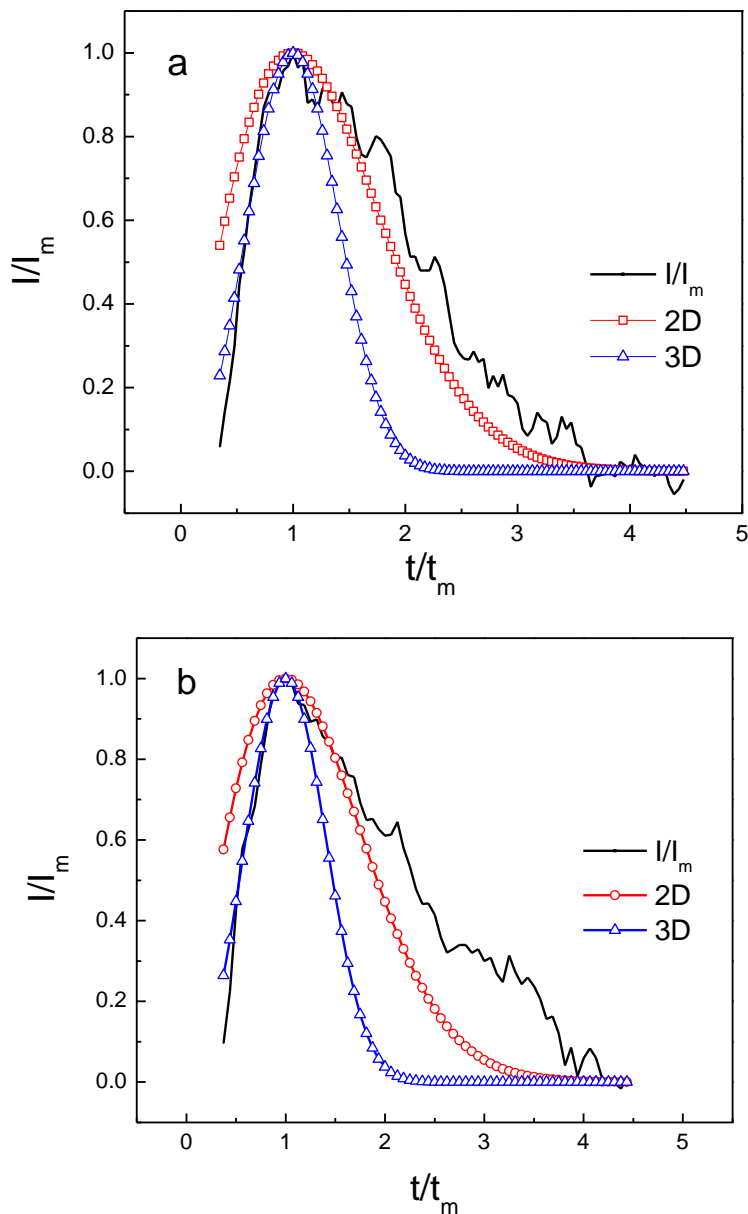
Figure 7. The non-dimensional i/i_m is plotted as a function of t/t_m, for the passive film formation of 316L SS with **(a)** and without **(b)** crevice.

Table 1. Analytical expressions of the survival probability function for various stochastic models.

	AK_1^2 ($mol^2cm^{-6}s^{-3}$)	K_2 ($A.cm^{-2}$)
Without crevice	8.621×10^{-5}	3.203×10^{-10}
With crevice	2.900×10^{-5}	2.733×10^{-10}

4.2. Effect of crevice on the corrosion initiation mechanism of 316L SS

Crevice corrosion initiation events takes place as a stochastic process [20], which have been analyzed by assuming various models including the series or parallel combination of an elemental birth stochastic process as well as the death stochastic process which had been reported before [27-31].

Table 2. Analytical expressions of the survival probability function for various stochastic models.

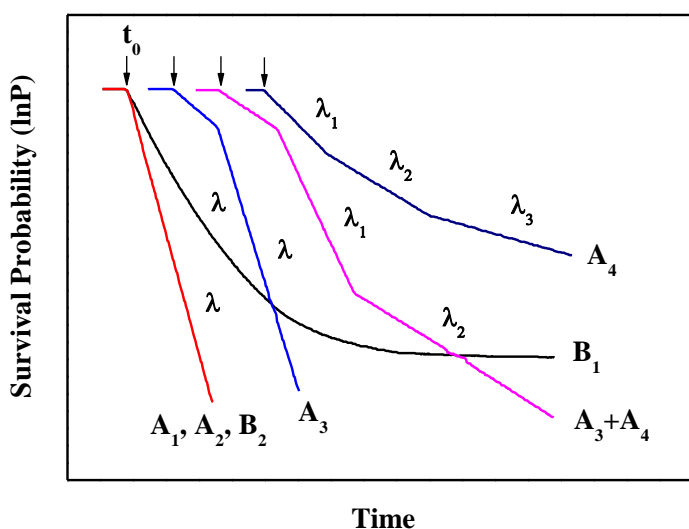| Model	Survival probability function

Birth process
  A1 simple
 	
  A2 series
 	
  A3 parallel
 	
  A4 combination
	$P_{sur}(t) = \exp[-\lambda(t-t_0)]$
	$P_{sur}(t) = \exp[-m\lambda(t-t_0)]$
	$P_{sur}(t) = 1 - \{1 - \exp[-\lambda(t-t_0)]\}^m$
	$P_{sur}(t) = \sum f_i \exp[-\lambda_i(t-t_0)]$

Birth and death process
  B1 parallel
 	
  B2 series
	$P_{sur}(t) = \mu/(\lambda+m) + \lambda/(\lambda+\mu)\exp[-(\lambda+\mu)(t-t_0)]$
	$P_{sur}(t) = \exp[-\alpha\lambda(t-\tau_c)\exp(-\mu\tau_c)]$

Figure 8. A schematic illustration of ln P_{sur} vs time of various stochastic models.

The expected equations for the survival probability, P_{sur}, and time for crevice corrosion initiation formulated for each model are shown in Table 2 and corresponding curves between ln(P_{sur}) and time are illustrated in Fig. 8. The survival probability should be defined as:

$$P_{sur} = 1 - \frac{i}{1 + N} \qquad (7)$$

where i is the order in the total number, N, the total number of measured induction time.

For deciding the exact model, the distribution of the induction time has to be fitted to a specific model by numerical or graphic simulation using the equations for an assumed model.
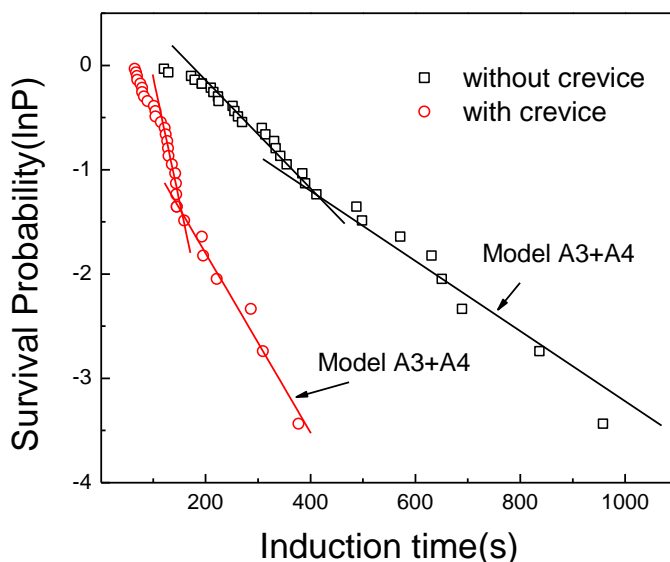

Figure 9. Plots of survival probability, P_{sur}, vs time for 316L SS with and without crevice.

Fig.9 was the plots of survival probability, P_{sur} vs induction time, for the crevice corrosion initiation of 316L SS with and without crevice. Both of the plots of the induction time distribution without crevice exhibited two linear regions. As introduced in the above paragraph, and considering many of the metastable corrosion transients were observed, this distribution type was the specific character of the combination of A3 model (parallel birth stochastic model) and A4 model (combination birth stochastic model). In the other word, the plots of the distribution of induction time with and without crevice exhibited analogue shape, which suggested that crevice did not change the corrosion initiation mechanism of 316L SS.

Localized corrosion initiation is modeled using a nonhomogeneous Poisson process [1, 32]. In this way, the distribution of corrosion induction times can be simulated using the Weibull distributions. Weibull distribution function is one of the widely used cumulative probability functions for predicting life time in reliability test [33]. This is because it can easily approximate the normal distribution, logarithmic normal distribution and exponential distribution functions. In addition, it is also possible to analyze data even when two or more failure modes are present at the same time. The cumulative probability $F(t)$ of a failure system can be introduced just as Weibull distribution function based upon a "weakest-link" model [4, 33, 34], which is expressed as

$$F(t) = 1 - \exp\left(-t^m / n\right) \qquad (8)$$

where m and n are the shape and scale parameters, respectively. From rearrangement of Eq. (8):

$$\ln\{\ln[1/(1 - F(t))]\} = m\ln t - \ln n \qquad (9)$$

By fitting Eq. (9) to the cumulative probability numerically calculated, two parameters m and n can be determined from the slope of the linear ln {ln [1/(1-$F(t)$)]} versus ln t plots and from the intercept on the ln {ln [1/(1- $F(t)$)]} axis, respectively.
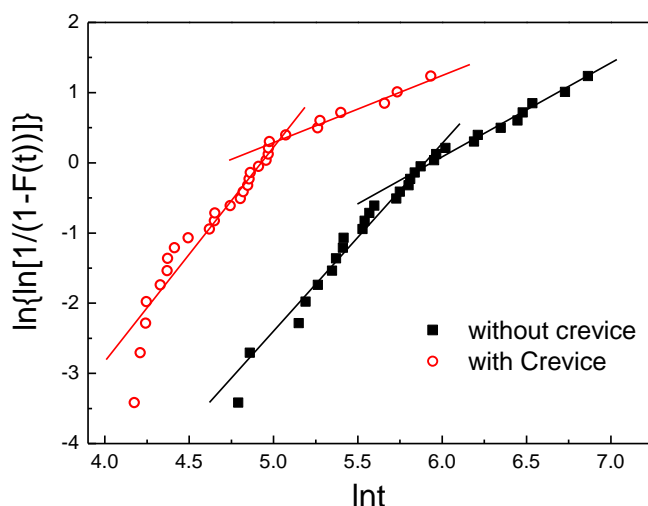

Figure 10. Weibull probability plots of 316L SS with and without crevice.

The Weibull probability plots for 316L SS with and without crevice were shown in Fig. 10. Both plots showed satisfactorily good two straight lines. These two slopes represent two limiting cases corresponding to corrosion initiation process dominant A3 model and A4 model, respectively. From Fig. 10, the values of m and n for corrosion initiation dominant by different stochastic model were quantitatively determined, which were listed in Table 3.

Table 3. Weibull distribution parameters for the corrosion initiation rate of 316L SS with and without crevice.

	model	m	n
Without crevice	A4	0.996	110.453
	A3	3.347	1.358×10^{-7}
With crevice	A4	0.932	77.033
	A3	3.330	1.256×10^{-7}

According to stochastic theory, it may be possible to predict the generation probability of events in the future from the past events. This is so-called "the conditional probability". Based upon a stochastic theory, Pyun et.al introduced the corrosion initiation rate [5-7], which is given by:

$$r(t) = \frac{m}{n} t^{m-1} \qquad (10)$$

The value of $r(t)$(/s) represents the rate of the corrosion initiation process dominant by different stochastic model in the next unit time for the specimens.
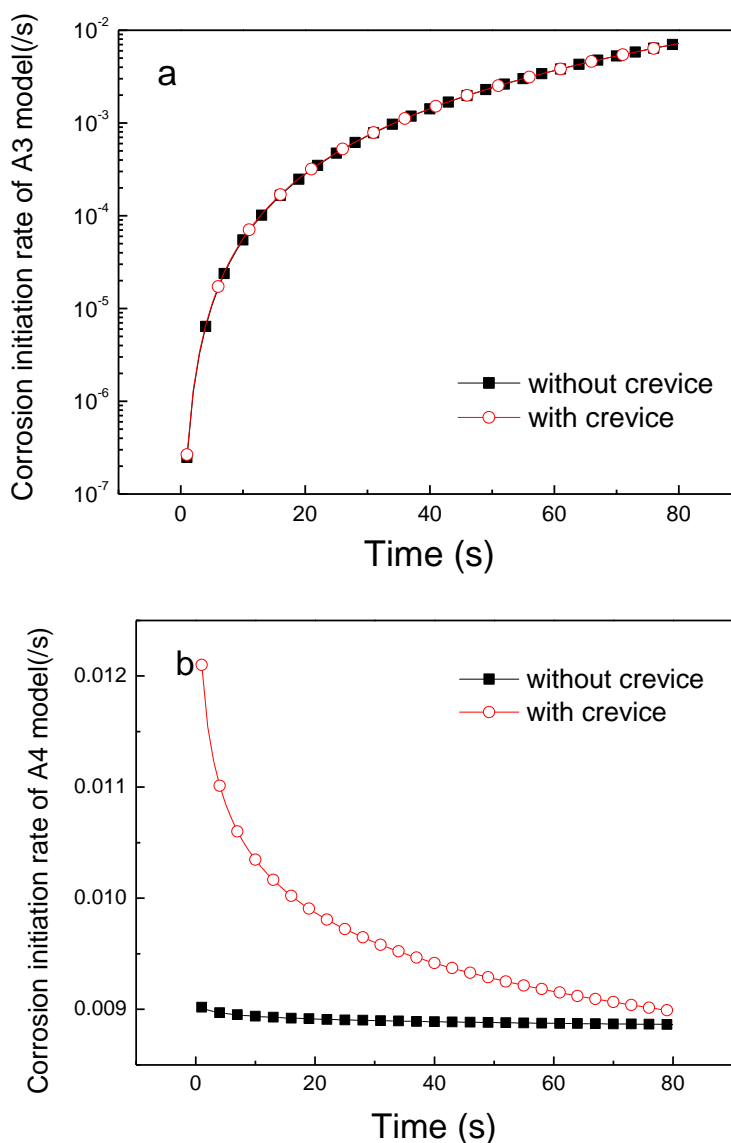

Figure 11. Plots of the corrosion initiation rate of 316L SS with and without crevice.

The rate $r(t)$ was determined by inserting the values of the shape and scale parameter m and n given in Table 3, into Eq. (10). The resulting rate for corrosion initiation, $r(t)$, was illustrated in Fig.

11. It was observed that the corrosion initiation rate of A4 model was increased in the presence of crevice, while, the corrosion initiation rate of A3 model showed independent with crevice.

During the last several decades, the mechanism of corrosion initiation of 316L SS could be grouped as [35]: permeation theory, breakdown of passive film theory and MnS inclusion theory. Pits in stainless steels are often associated with MnS inclusions.

Because all the samples were cut from the same rod, the MnS inclusion size and its distribution of each sample should be same in maco-scale. This indicated that the corrosion initiation rate generated by the dissolution of MnS was independent with crevice. Combining Fig.11 a results, it suggested that the A3 model (parallel birth stochastic model) was associated with the dissolution of MnS inclusion.

The section 4.1 indicated that the formation rate of passive film decreased in case of crevice. In the view of film breakdown theory, the passive film covered by crevice was easier to be brokendown, which implied that crevice increased the corrosion initiation rate obeyed film breakdown mechanism. Considering the result Fig.11 b, the A4 model (combination birth stochastic model) could be assumed as the breakdown process of passive film.

4.3. Effect of crevice on the growth of stable corrosion of 316L SS

After a sudden current rise, the stable corrosion occurred and grew. Fig. 12 illustrated an example of potentiostatic current trace at a constant potential of $90mV_{Ag/AgCl}$.
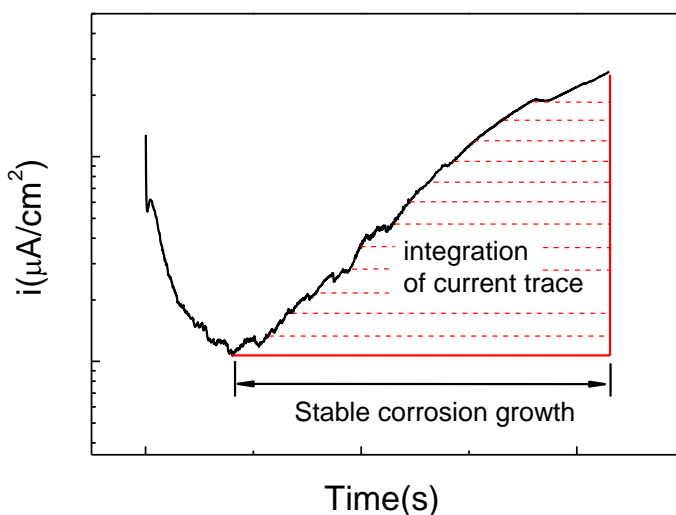

Figure 12. Scheme about the determine method of stable corrosion growth rate.

The integrated area of the marked zone by dash-line denotes the charges (Q) which were consumed during corrosion growth process. Stable corrosion growth rate (v) can be illustrated as Q/t, where t is stable corrosion growth time.

Gumbel distribution of stable corrosion growth rate described the relationship between *v* and the reduced variant (*Y*). The values of the reduced variant (*Y*), was calculated according to Eq. (11) [36].

$$Y = -\ln(-\ln(1 - \frac{i}{N+1})) = \frac{1}{\alpha}v_i - \frac{\mu}{\alpha} \qquad (11)$$

Where *N* denotes the total repeated times of the measurements of *v*, *i* is the order of the measured values of *vi* when they are ranked from lower value to higher value (*i* = 1, 2, 3, …, *N*), *μ* is the central parameter (the average value of the maximum *v*) and *α* is the scale parameter, which defines the width of the distribution.
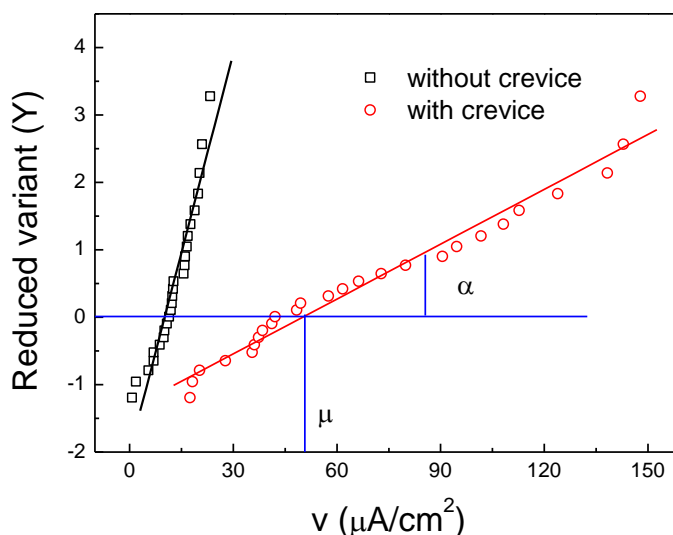

Figure 13. Gumbel probability plots of 316L SS with and without crevice.

Fig. 13 showed the Gumbel distribution of stable corrosion growth rate for 316L SS with and without crevice. The character of stable corrosion growth rate distribution for both plots indicated one line segment. *μ* and *α* can be obtained (Table 4) by fitting these line segments.

Table 4. Gumbel distribution parameters for 316L SS with and without crevice.

	α (μm)	μ (μm)
Without crevice	8.666	15.494
With crevice	4.665	7.101

Then, the probability of stable corrosion growth rate (*P*) can be obtained according to Gumbel Type extreme value distribution by the following:

$$P = 1 - \exp[-\exp(-\frac{v_i - \mu}{\alpha})] \qquad (12)$$

Fig. 14 showed the relationship between the probability of stable corrosion growth rate (P) and v for 316L SS with and without crevice, respectively, according to Eq. (12). At a certain corrosion growth rate, the probability for 316L SS with crevice was higher than that without crevice.
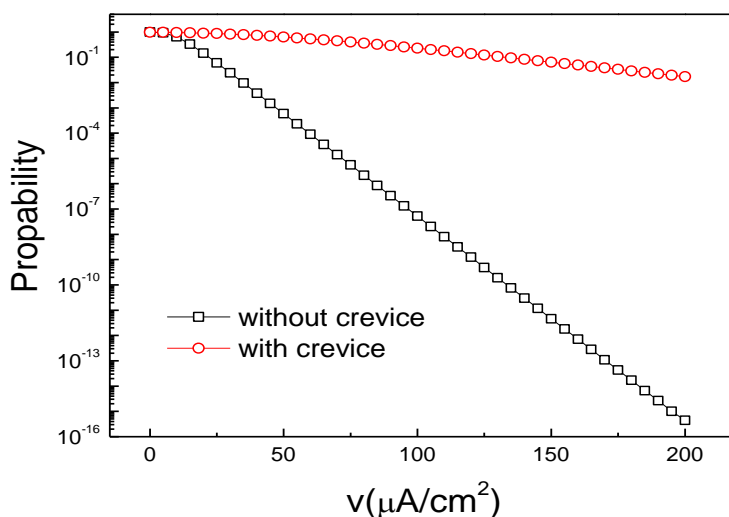

Figure 14. Probabilities of various stable corrosion growth rate occurring with and without crevice.

The corrosion growth process was determined by the localized chemistry environment [35]. The electrolyte in pit cavity was characterized as low pH, high metal ion and chloride content. The cavity electrolyte was near the saturation, even super-saturation and deposited on the cavity interface. Such aggressive electrolyte was maintained by the diffusion process. Once the lacy was brokendown, the aggressive cavity electrolyte would be diluted by bulk solution, and then the pit growth process was terminated. In the presence of crevice, the bulk solution was difficult to diffuse into the crevice and dilute the crevice solution, thus, the crevice solution was acidification with the oxygen depletion. Although the breakdown of lacy, the cavity electrolyte could not be diluted by crevice solution, which indicated the corrosion was easy to grow up with a higher growth rate, and finally developed into a stable corrosion cavity and spread over the covered surface.

5. CONCLUSION

The results revealed that crevice increased the corrosion susceptibility of 316L SS.

The nature of the passive film formation followed progressive nucleation (3D) mechanism. The presence of crevice had no effect on the passive film formation mechanism, but hindered the formation rate of the passive film.

The corrosion initiation mechanism was the combination of A3 model (dissolution of MnS inclusion) and A4 model (passive film breakdown). The presence of crevice had no influence on the dissolution of MnS inclusion, however, accelerated the breakdown of passive film.

The presence of crevice increased the stable corrosion growth probability. In case of crevice, the stable corrosion was easy to grow up with a higher growth rate, and finally developed into a larger corrosion cavity and spread over the covered surface.

References

1. A.Valor, F. Caleyo, L. Alfonso, D. Rivas, *J. Hallen Corros. Sci*, 49 (2007) 559
2. Y. Tsukaue, G. Nakao, Y. Takimoto, K. Yoshida, *Corros*, 50 (1994) 755
3. T. Shibata, *Corros,* 52 (1996) 813
4. J. Park, S. Pyun, *Corros. Sci*, 46 (2004) 285
5. K. Na, S. Pyun, *Electrochim. Acta*, 52 (2007) 4363
6. K. Na, S. Pyun, *Corros. Sci*, 49 (2007) 2663
7. K. Na, S. Pyun, *Corros. Sci*, 50 (2008) 248
8. G. Ilevbare, G. Burstein*, Corros. Sci,* 43 (2001) 485
9. G. Burstein, S. Vines, *J. Electrochem. Soc*, 148 (2001) B504
10. G. Burstein, R. Soutob, *J. Electrochem. Soc*, 151(2004) B537
11. J. Provan, E. Rodriíguez, *Corros*, 45(1989) 178
12. P. Aziz, *Corros*, 12 (1956) 495
13. H. Hong, *Corros,* 55 (1999) 10
14. F. Bolzoni, P. Fassina, G. Fumagalli, L. Lazzari, E. Mazzola, *Metallurg Ita*, 98(2008) 9
15. T. Zhang, X. Liu, Y. Shao, G. Meng, F. Wang, *Corros. Sci*, 50 (2008) 3500
16. G. Meng, L. Wei, T. Zhang, Y. Shao, F. Wang, *Corros. Sci*, 51 (2009) 2151
17. Y. Shao, J. Cao, T. Zhang, G. Meng, F. Wang, *Corros. Sci,* 51 (2009) 371
18. J. Oldfield, W. Sutton, *Br. Corros. J*, 13 (1978) 13
19. J. Oldfield, W. Sutton, *Br. Corros. J*, 15(1980) 31
20. S. Fujimoto, T. Shibata, M. Minamida, S. Udaka, *Corros. Sci*, 36(1994) 1575
21. ASTM Stand G48-97, "Pitting and crevice corrosion resistance of stainless steel and related alloy by using ferric chloride solution" ASTM International, West Conshohocken, PA, (1998).
22. M. Holzle, U. Retter, D. Kolb, *J. Electroanal. Chem*, 371 (1994) 101
23. E. Budevski, G. Staikov, W. Lorenz, *Electrochim. Acta* 45(2000) 2559
24. M. Jafarian, F. Gobal, I. Danaee, R. Biabani, M. Mahjani, *Electrochim. Acta*, 53 (2008) 4528
25. F. Varela, E. Codaro, J. Vilche, *J. Appl. Electrochem*, 27 (1997) 1232
26. R. Armstrong, M. Fleischmann, H. Thirsk, *J. Electroanal. Chem*, 11(1966) 208
27. T. Shibata, T. Takeyama, *Nature*, 260(1976) 315
28. T. Shibata, Y. Zhu, *Corros. S*ci, 36 (1994) 153
29. T. Shibata, M. Ameer, *Corros. S*ci, 33(1992) 1633
30. T. Shibata, Y. Zhu, *Corros. Sci*, 36 (1994) 1735
31. T. Shibata, Y. Zhu, *Corros. Sci*, 37 (1995) 853
32. G. Engelhardt, D. Macdonald, *Corros. Sci*, 46 (2004) 2755

33. E. Lewis, "Introduction to Reliability Engineering", John Wiley and Sons, New York (1987).
34. S. Pyun, E. Lee, G. Han, *Thin Solid Film*, 239 (1994) 74
35. G. Frankel, *J. Electrochem. Soc*, 145 (1998) 2186
36. A.Trueman, *Corros. Sci*, 47(2005) 2240